

VIGFace: Virtual Identity Generation for Privacy-Free Face Recognition

Minsoo Kim*

Korea Institute of Science and Technology
Korea National University of Science and Tech.
Seoul, Korea

kim1102@kist.re.kr

Gi Pyo Nam

Korea Institute of Science and Technology
Korea National University of Science and Tech.
Seoul, Korea

gpnam@kist.re.kr

Min-Cheol Sagong*

Korea Institute of Science and Technology
Seoul, Korea

mcsagong@kist.re.kr

Junghyun Cho

Korea Institute of Science and Technology
Korea National University of Science and Tech.
Yonsei-KIST Convergence Research Institute
Seoul, Korea

jhcho@kist.re.kr

Ig-Jae Kim

Korea Institute of Science and Tech.
Yonsei-KIST Convergence Research Institute
Seoul, Korea

drjay@kist.re.kr

Abstract

Deep learning-based face recognition continues to face challenges due to its reliance on huge datasets obtained from web crawling, which can be costly to gather and raise significant real-world privacy concerns. To address this issue, we propose **VIGFace**, a novel framework capable of generating synthetic facial images. Our idea originates from pre-assigning virtual identities in the feature space. Initially, we train the face recognition model using a real face dataset and create a feature space for both real and virtual identities, where virtual prototypes are orthogonal to other prototypes. Subsequently, we generate synthetic images by using the diffusion model based on the feature space. The diffusion model is capable of reconstructing authentic human facial representations from established real prototypes, while synthesizing virtual entities from devised virtual prototypes. Our proposed framework provides two significant benefits. Firstly, it allows one to create virtual facial images without concerns about privacy and portrait rights, guaranteeing that the generated virtual face images are clearly differentiated from existing individuals. Secondly, it serves as an effective augmentation method by incorporating real existing images. Further experiments

demonstrate the superiority of our virtual face dataset and framework, outperforming the previous state-of-the-art on various face recognition benchmarks.

1. Introduction

Deep learning-based Face Recognition (FR) models have significantly improved their performance due to recent advances in network architectures [14, 15, 18, 23, 42, 44] and enhancements in loss functions [7, 25, 29, 39, 40, 52]. The latest FR models utilize the softmax-variant loss for training to reduce intra-class variance and increase inter-class separability in the embedding space. This necessitates a very large dataset with numerous distinct individuals, significant variations within each individual for intra-class variance, and precise labels of subject identities (IDs). However, datasets are typically collected through web-crawling and then refined using automatic techniques that employ FR logits [9, 58]. Although this approach is successful in eliminating mislabeled data, it still struggles with persistent issues of small intra-class variance. Moreover, in the face recognition field, unlike other ordinary image classifications, there are practical issues such as portrait rights, making it even more difficult to collect training data. For instance, datasets such as those referenced in [13, 54, 58]

*These authors contributed equally to this work

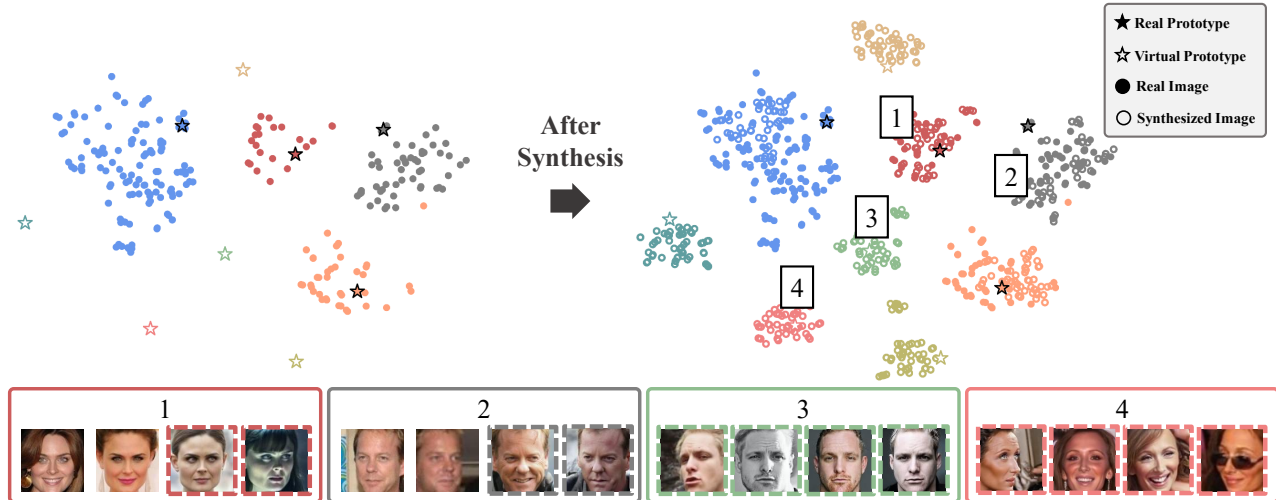


Figure 1. T-distributed Stochastic Neighbor Embedding (T-SNE) [49] plot of embeddings from real and synthesized images. The filled and lined stars represent the real and virtual prototypes, while filled and lined circles indicate the embeddings of real and synthesized images, respectively. The bottom of the figure shows the face images included in the cluster, and the dotted outlined images represent the face images generated using our method.

consist of images of celebrities collected from the internet without consent. Furthermore, the datasets mentioned in [24, 36] include facial images of the general population, including children. Due to privacy concerns, public access to these datasets has been revoked [50].

Synthetic datasets have been employed to address limitations caused by a scarcity of real datasets [6, 22, 47] and biases present in the available real datasets [17, 48]. In the realm of face recognition, artificial faces show promise in addressing the aforementioned issues related to real face datasets. Generated faces are at low risk for label noise due to conditional generation. Bias problems, such as long-tailed distributions, which lead to class imbalances, can be mitigated by data augmentation. Importantly, there are no privacy concerns with virtual identities facial images if the method is effective. Therefore, when creating artificial datasets, it is essential to consider: 1) ensuring that the generated data mirror the real data distribution, 2) the ability to generate new subjects separated from real data, and 3) maintaining ID consistency for each subject.

Previous attempts to create artificial face datasets have addressed some of the three aspects individually, but to the best of our knowledge, none have simultaneously taken into account all three aspects [2, 4, 26, 38]. SynFace [38] introduces a high-quality synthetic face image dataset, closely reminiscent of real face images, using DiscoFaceGAN [11]. However, DiscoFaceGAN is only capable of generating a limited number of unique subjects, fewer than 500 [26]. On the other hand, DigiFace [2] utilizes 3D parametric modeling to create synthetic face images of various subjects. However, it faces difficulties in accurately replicating the

quality and style distribution observed in real face images. DCFace [26] proposes a diffusion-based method to generate data that can produce a large number of novel subjects, maintain the style of real datasets, and ensure label consistency. However, DCFace primarily focuses on creating synthetic data rather than increasing the capabilities of data augmentation. IDiffFace [4] utilized identity-conditioned latent diffusion to synthesize facial images from FR feature representations. However, they were unable to guarantee the uniqueness of the synthesized identities, since they randomly sampled the synthetic FR features.

We present a novel approach for generating face data that enhances both intra-class variance and inter-class diversity. The main concept of our paper is to incorporate virtual prototypes into the FR model. The diffusion model is trained to preserve the identity of the individuals when generating face images based on the FR embedding. Since virtual prototypes are orthogonal to other prototypes, virtual subjects are guaranteed to be distinguished from the original data. Fig. 1 shows a toy example that visualizes the embeddings of real and virtual subjects to demonstrate the effectiveness of the suggested method. The virtual embedding can be distinct from the real individual clusters, whereas the images generated from virtual prototypes form unique clusters. The visualization demonstrates that our framework generates distinctive virtual human faces with high consistency in ID. The proposed method effectively addresses privacy concerns by creating datasets of non-existent individuals and achieving state-of-the-art performance compared to models trained with previous virtual person generation methods. Additionally, the FR model, which was trained

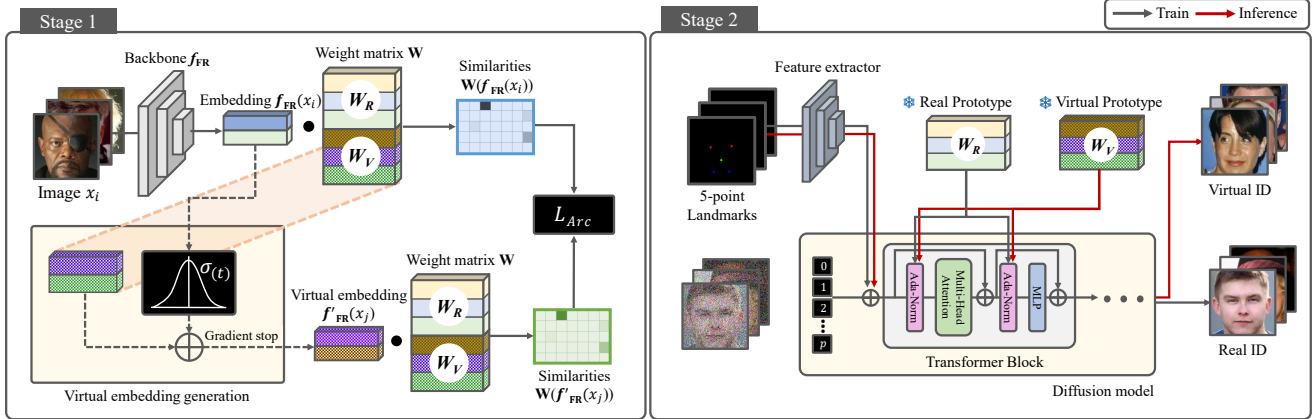


Figure 2. Pipeline for the proposed method. Conventional FR training includes prototypes for only real individuals, indicated as W_R . We add k prototypes for virtual IDs, denoted as W_V . The virtual embedding $f'_{FR}(x_j)$ corresponding to the virtual person ID: j is generated to follow distribution of the real embeddings. To synthesize the facial image from virtual prototypes, we adopt the DiT architecture [37], following the design approach of the Vision Transformer (ViT) [12]. Additionally, we adjust the DiT model to utilize 5-point landmark images to handle pose variations.

using a combination of real and synthetic images together, achieves better performance than the model trained using only real images. This shows that the proposed method is also superior from the perspective of a data augmentation method.

Our contribution can be summarized as follows:

- Introducing VIGFace, a method designed to generate virtual identities with realistic appearance, guided by three main criteria: generating novel subjects that are not found in the real-world, consistently preserving the identity, but ensuring diverse characteristics for each individual.
- Showing that the synthetic data generated by VIGFace can leverage intra-class diversity and inter-class variance, achieving SOTA performance in face recognition.
- Releasing the first virtual-only face dataset that can fully substitute the real dataset, helping alleviate privacy concerns.

2. Related work

2.1. Face Recognition Models

Current state-of-the-arts (SOTA) FR methods, such as [3, 7, 10, 21, 25, 29, 34, 51], are designed based on softmax loss but particularly utilize the angular/cosine distance instead of the Euclidean distance. The goal of these methods is to maximize the similarity between the embeddings and the ground-truth (GT) prototype, while minimizing the similarity between the embedding and prototypes of other classes. As a result, all embeddings in the same class, including prototypes, converge while maintaining their maximum distance from other classes. Therefore, if the embedding dimension is large enough, the clusters of each class will be nearly orthogonal [7]. Naturally, a larger dataset

that contains a greater variety of images allows for the training of better-performing FR models. Therefore, over time, larger and more diverse datasets [1, 13, 19, 58] have been collected and published in the academic field. However, issues such as portrait rights and the high cost of building large-scale data remain unresolved.

2.2. Synthetic Face Image Generation

Synthetic training datasets have demonstrated advantages in areas such as face recognition [2, 38] and anti-spoofing [30, 45]. They can address issues like class imbalance, informed consent, and racial biases, which are often found in conventional large-scale face datasets [2, 7, 38]. Additionally, synthetic datasets support the importance of ethical considerations, such as portrait rights. Despite their benefits, the use of synthetic datasets lacks widespread acceptance, causing reduced recognition accuracy when used as the only training data.

SynFace [38] proposed a method that uses DiscoFaceGAN [11] to synthesize the virtual faces. DigiFace-1M [2] suggested 3D model-based face rendering with image augmentations to create virtual face data and showed that the FR model could be trained using only virtual face images. DCFace [26] proposed a diffusion-based face generator combining subject appearance (ID) and external factor (style) conditions. IDiffFace [4] utilized FR identity conditioned latent diffusion to generate synthetic image from FR feature representation. Furthermore, GandiffFace [33] utilized the GAN the identity feature generation. Although the above images have succeeded in reducing the dependence on images crawled from the web, there is still a performance gap between the FR model trained on real training datasets and the FR model

trained on synthetic training datasets. We proposed a data augmentation method that can generate the virtual ID with high intra-class variance and a large number of unique individuals, thereby aiding in FR model training.

3. Methods

Our framework comprises two stages. First, we train the FR model using the real face dataset and design the feature space for both real and virtual IDs. Second, synthetic images are generated using the diffusion model based on the feature space of the pre-trained FR model that was trained in the first stage. This section provides a detailed explanation of each stage of the proposed framework.

3.1. Stage 1: FR Model Training

The proposed framework begins with training the FR model using real face images. This stage serves two purposes: 1) Training the FR model to achieve prototype features from face images, which are necessary for training the diffusion model in the second stage, and 2) Simultaneously assigning the positions of both the real ID and the virtual ID on the feature space. We choose ArcFace [7] to train the FR model in this stage. The ArcFace loss used to train the FR backbone f_{FR} and the prototype $W = [w_1, w_2, \dots, w_n]$ can be described as follows:

$$L_{\text{arc}} = -\log \frac{e^{s \cos(\theta_{y_i} + m)}}{e^{s \cos(\theta_{y_i} + m)} + \sum_{j=1, j \neq y_i}^n e^{s \cos \theta_j}}, \quad (1)$$

$$\cos \theta_j = \frac{w_j^T f_{\text{FR}}(x_i)}{\|w_j\| \|f_{\text{FR}}(x_i)\|}, \quad (2)$$

where n denotes the total number of real IDs, while m and s represent the margin and scale hyperparameters, respectively. With conventional FR training methods, only prototypes for real individuals, which can be denoted as $W_R = [w_r^1, w_r^2, \dots, w_r^n]$, are necessary for training. However, in our work, we include additional k prototypes for virtual IDs, denoted as $W_V = [w_v^1, w_v^2, \dots, w_v^k]$, which are used to generate facial images of nonexistent individuals in the real world. As a result, the prototype is defined as a linear transformation matrix $W \in \mathbb{R}^{(n+k) \times D}$, where D refers to the dimension of the embedding features.

However, due to the absence of a face image for virtual IDs, their prototypes cannot be updated to maximize the distance from each other with L_{arc} . Consequently, all virtual prototypes converge to a single point in the feature space when trained with the original L_{arc} as shown in Fig. 3a. To address this problem, we propose to use virtual feature embedding $f'_{\text{FR}}(x_j)$ to update the virtual prototypes w_v^j . The virtual embedding $f'_{\text{FR}}(x_j)$ corresponding to the virtual person ID: j was generated as follows:

$$f'_{\text{FR}}(x_j) = w_v^j + \mathcal{N}(0, 1) \cdot \sigma, \quad (3)$$

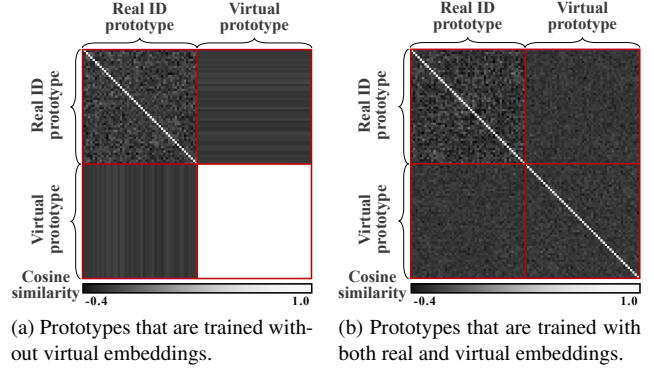


Figure 3. Changes in the cosine similarity matrix of the prototypes from our method. Similarity values were min-max normalized.

$$\sigma^2 = \frac{1}{b} \sum_{i=1}^b (f_{\text{FR}}(x_i) - w_r^i)^2, \quad (4)$$

where b refers the mini-batch size. As can be seen from the equations, the virtual embedding $f'_{\text{FR}}(x_j)$ follows a distribution in which the standard deviation matches that of the real embeddings. The aggregate loss L_{arc} is calculated simultaneously using both the real embedding $f_{\text{FR}}(x)$ and the virtual embedding $f'_{\text{FR}}(x)$, allowing the virtual prototype w_v^j to maintain minimal similarities with other prototypes, as illustrated in Fig. 3. Note that generating the virtual embedding process is not necessary for the backward process. Since batch configuration affects the calculated standard deviation, we utilize the exponential moving average (EMA) to reduce this influence. The corrected standard deviation σ for the current iteration t is calculated as follows:

$$\sigma = \sigma_{(t)} \cdot \alpha + \sigma_{(t-1)} \cdot (1 - \alpha). \quad (5)$$

The hyperparameter α is set to 0.9. The number of virtual embedding, b_v is determined based on the mini-batch size b_r , the number of virtual ID prototypes k , and the number of real ID prototypes n . In our study, we set $b_v = (k \times b_r) / n$ so that both real and virtual prototypes can be updated evenly.

The overall pipeline of this stage is illustrated in Fig. 2. Note that gradients for virtual embedding have no effect on the backbone. We confirm that the similarity distribution between the virtual prototypes closely resembles the similarity distribution between the real prototypes as shown in Fig. 3b.

3.2. Stage 2: Face Generation with Diffusion Model

The next step is to synthesize face images using the diffusion model. To obtain the training dataset for the diffusion model, we utilize the FR model, which involves collecting pairs of images x_0 and their corresponding prototypes w_r . The input to our diffusion model includes the timestep t ,

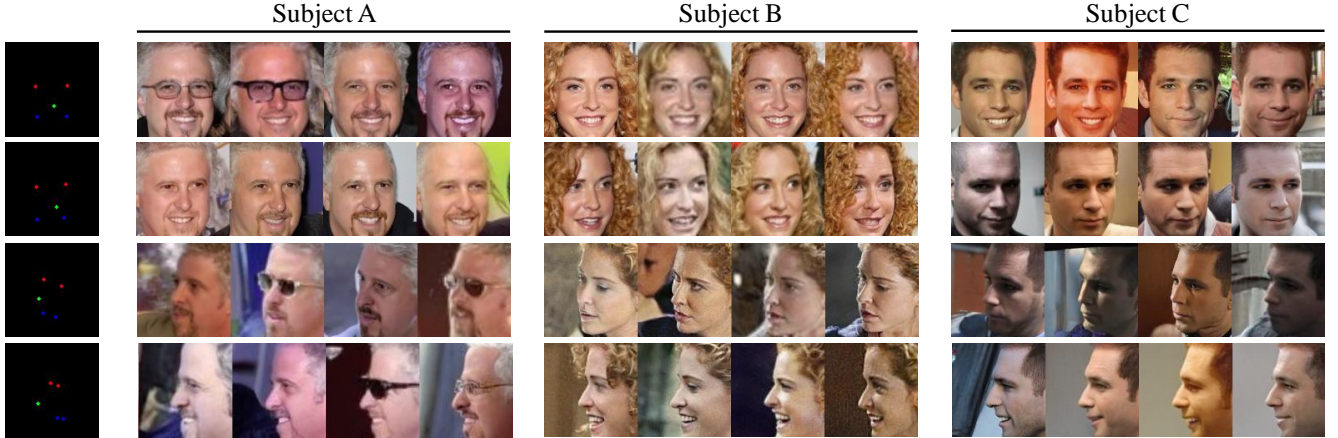


Figure 4. Virtual face generated in VIGFace (B). Each row lists facial images in different pose environments created using five facial landmarks. Our method can generate various conditions of face images, such as illumination, occlusion by accessories, and facial expressions, while controlling the pose variations of the face images.

the FR prototype vector w_r , five facial landmarks image y , and the noisy image x_t . In line with the approach proposed in the previous method [28], our model predicts velocity v_t rather than noise ϵ injected into x_t . We adopt the DiT architecture [37] using the design approach of the visual transformer (ViT) [12]. We modify the DiT model by incorporating the five facial landmarks (including the left eye, the right eye, the nose, the left mouth corner, and the right mouth corner) [55] image. The five facial landmark images are acquired using RetinaFace [8], and employed as conditions to account for pose variations. Fig. 4 shows the synthesized face images conditioned by five facial landmarks. The first column lists input landmark conditions in different pose environments. As illustrated in the figure, the proposed model is capable of producing a wide range of styles (like hair, glasses, and lighting) while also delivering various pose variations, all with a high degree of consistency. In order to achieve both the generation of facial images and the synchronization of their feature space on the FR model, our diffusion model incorporates a constraint which aims to minimize the feature distance between the original image and the input prototypes as follows:

$$\min_{\theta} \mathbb{E}_{\epsilon, t} \|f_{\text{FR}}(\hat{x}_{\theta}(x_t, t, w_r, y)) - w_r\|_2^2. \quad (6)$$

We adopt classifier-free guidance [16] by randomly assigning zero values to condition embeddings, w_r , 10% of time. Sampling is performed as follows:

$$\tilde{x}_{\theta}(x_t, t, W, y) = \alpha \cdot x_{\theta}(x_t, t, W, y) + (1 - \alpha) \cdot x_{\theta}(x_t, t, y), \quad (7)$$

where $x_{\theta}(x_t, t, w_r, y)$ and $x_{\theta}(x_t, t, y)$ are conditional and unconditional x_0 -prediction, respectively and α is *guidance weight*.

4. Experiments

We analyze our framework from two perspectives. Firstly, by training the FR model exclusively with facial images generated for virtual IDs, we demonstrated the capability of our model to serve as a viable alternative to real face datasets, addressing concerns such as label noise or privacy. Secondly, we train the FR model using both real images and generated face images simultaneously, showcasing the potential of our model as a data augmentation framework for face recognition.

4.1. Implementation Details

For stage 1: We use a modified ResNet-50 [7] and ArcFace [7] to train the face recognition (FR) backbone. The CASIA-WebFace [19] dataset serves as the training data. Following the alignment method in [29], the facial images are aligned to a resolution of 112×112 . After alignment, the pixel values are normalized, with both the mean and standard deviation set to 0.5. We set the mini-batch size for the real dataset to 512 and use Stochastic Gradient Descent (SGD) as the optimizer, with a weight decay of $5e-4$ and momentum of 0.9. The initial learning rate is set to 0.1 and divided by 0.1 at the 24th, 30th, and 36th epochs, with training concluding at the 40th epoch. The ArcFace hyperparameters for the margin m and the scale factor s are set to 0.5 and 30, respectively.

For stage 2: To generate synthetic face images, we explore the best setting for the diffusion model. To facilitate comparison, we utilized the widely adopted DiT-B model for all experiments. Since the traditional FR model typically employs a resolution of 112×112 for face images, we set the window size of the DiT patch extractor to 4. We

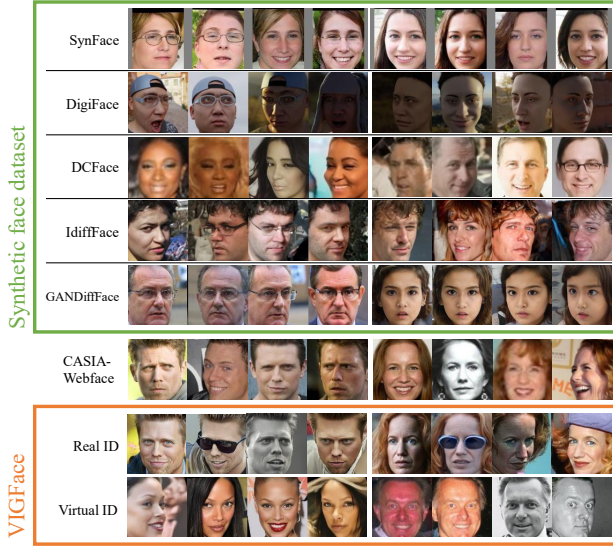


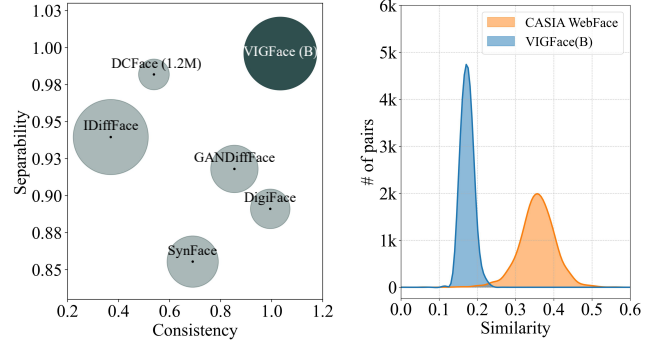
Figure 5. Comparison of the generated virtual ID images with the conventional methods [2, 4, 26, 33, 38] and our methods that are trained on CASIA-WebFace. For each synthetic dataset, we present two subjects in a single row.

follow the publicly released implementation of DDIM [43] with the cosine noise scheduler [5]. Following the approach of the previous method [28], we employ the enforced zero terminal SNR and trailing timesteps. The diffusion model is trained for 5M iterations with a batch size of 512 using AdamW Optimizer [27, 31] with a learning rate of $1e-4$. For sampling, we use classifier-free guidance implementation [16] in 50 timesteps.

4.2. Virtual Identity Generation

Since diffusion models focus on optimizing the visual aspect with input conditions, they tend to produce images that are high in consistency but lack of variance. One simple way to achieve a balance between consistency and variance is by adjusting the classifier-free guidance weight scale. Higher guidance enforces stronger conditioning of input labels. In other words, it results in more constant images but slightly similar samples. We observe that the proposed model performs best as the scale becomes $w = 4.0$.

We construct a toy example visualizing the feature space consists of three real persons and five virtual persons to demonstrate the efficacy of the synthesized images in Fig. 1. As seen in the figure on the left, the virtual embedding optimization obviously provides separable virtual prototypes from real individual clusters. The figure on the right illustrates that our synthesized images enforce high variance to the dataset. Synthesized images of real individuals filling the gap in the cluster provide intra-class variance to the subjects. Additionally, the cluster of generated images from virtual prototypes, while staying separate from other sub-



(a) The normalized properties of various synthetic datasets. The sizes of the circles indicate the intra-class diversity. (b) Cosine similarity with the most similar negative class center in the real dataset (CASIA-WebFace).

Figure 6. Properties of VIGFace compared with those of synthesized datasets generated by previous methods.

jects, demonstrates the effectiveness of our framework for generating unique virtual human faces in high consistency.

Fig. 5 shows the qualitative comparison of conventional synthetic datasets and the proposed VIGFace. As shown in the figure, the facial images generated using the VIGFace model show remarkable uniformity in generating consistent virtual individuals, while also incorporating variations such as hair styles, accessories, makeup, and expressions. It is important to emphasize that the key characteristic of a training dataset to achieve a high-performance FR model is not the high quality of the images themselves, but rather the high consistency and variance of the generated facial images belonging to the same person.

Property of generated Dataset To compare the properties of the synthetic face datasets, we measured the 1) class consistency, 2) class separability, and 3) intra-class diversity of generated images. The class consistency reflects the uniformity of the samples in the same label condition. Consequently, the consistency of class k (C_k) was measured as follows:

$$C_k = \frac{1}{N^2} \sum_{j=1}^N \sum_{i=1}^N \frac{f(x_i) \cdot f(x_j)}{\|f(x_i)\| \|f(x_j)\|}, \quad (8)$$

where N is the number of images in a class k . Higher class consistency means that the samples are more uniform under the same label.

We also measured the class separability to assess the integrity of the dataset; in other words, to ensure that all subjects in the dataset are unique. The class separability for a class k (S_k) is measured as the average distance between the center of class k and the centers of the negative classes,

Training Dataset	# of Images (classes \times variations)	Verification Benchmarks					IJB Benchmarks		
		LFW	CFP-FP	CPLFW	AgeDB	CALFW	Avg.	IJB-B	IJB-C
CASIA-Webface (Real)	0.49M ($\approx 10.5K \times 47$)	99.30	96.41	88.88	94.25	92.57	94.28	78.71	83.44
SynFace	0.5M ($10K \times 50$)	86.03	71.73	65.53	62.75	69.88	71.18	15.37	17.60
DigiFace	1.2M ($10K \times 72 + 100K \times 5$)	87.15	76.37	66.80	61.55	69.18	72.21	15.57	20.36
DCFace (0.5M)	0.5M ($10K \times 50$)	96.37	80.06	77.38	83.58	86.62	84.80	56.73	60.29
DCFace (1.2M)	1.2M ($20K \times 50 + 40K \times 5$)	98.42	86.37	82.13	90.25	90.88	89.61	73.11	76.49
IDiffFace	0.5M ($10K \times 50$)	95.38	76.56	77.22	79.35	86.22	82.95	27.02	32.36
GANDiffFace	0.5M ($10K \times 50$)	90.77	73.27	72.32	66.35	74.68	75.48	34.85	39.94
VIGFace (S)	0.5M ($10K \times 50$)	98.60	94.74	85.47	88.60	88.52	91.19	62.22	69.27
VIGFace (B)*	1.2M ($20K \times 50 + 40K \times 5$)	99.10	96.47	88.82	92.32	92.15	93.77	72.68	78.85
VIGFace (B)	1.2M ($60K \times 20$)	99.15	96.66	88.88	92.73	92.22	93.93	74.91	80.50

Table 1. FR benchmark results trained with various virtual face datasets. The 1:1 verification accuracies (%) for five benchmarks are provided. Our method is specified by the number of images as small (S) and base (B). FR backbone is IR-SE50 + ArcFace [7]. * indicates a long-tailed data that aligns the subject distribution with the previous method, DCFace. **Bold** indicates the best.

Training Dataset	Backbone	Method	Average Accuracy	IJB-C
CASIA-Webface	R50	Arc.	94.28	83.44
DCFace (1.2M)	R50	Arc.	89.61	76.49
	R50	Ada.	90.70	81.63
	R100	Arc.	89.87	75.87
	R100	Ada.	90.97	82.02
VIGFace (B)	R50	Arc.	93.93	80.50
	R50	Ada.	94.14	81.31
	R100	Arc.	94.35	80.63
	R100	Ada.	94.56	81.56

Table 2. FR benchmark results that obtained using various implementations. For the table, different backbones (IR-SE50, IR-SE100) and methods (ArcFace, AdaFace) were utilized for training. The average accuracy (%) for five benchmarks [20, 35, 41, 56, 57] and the IJB-C results at TAR@FAR=1e-4 are provided.

as follows:

$$S_k = \frac{1}{K-1} \sum_{i=1, i \neq k}^K 1 - \frac{\bar{f}_k \cdot \bar{f}_i}{\|\bar{f}_k\| \|\bar{f}_i\|}, \quad (9)$$

where K is the number of classes. \bar{f}_k represents the class center obtained by averaging the embedding vectors of the images that belong to class k . As shown in the formula, a high S_k indicates that the images are distinct from the negative classes.

The intra-class diversity measures how various the conditions of samples are under the same label. Various conditions, such as pose, low light, and occlusions, make face recognition more challenging. Motivated by this observation, we calculated the intra-class diversity of a class k (D_k) using the variance of Face Image Quality Assessment (FIQA) scores as follows:

$$\overline{\text{FIQA}}_k = \frac{1}{N} \sum_{i=1}^N \text{FIQA}(x_i), \quad (10)$$

$$D_k = \frac{1}{N} \sum_{i=1}^N (\text{FIQA}(x_i) - \overline{\text{FIQA}}_k)^2, \quad (11)$$

where $\text{FIQA}(x_i)$ indicates the SER-FIQ score [46] of the generated image x_i .

The scores C_k , S_k , and D_k , are derived from a pre-trained ArcFace model that was trained using the Glint-360K dataset. Fig. 6a shows the average values of the properties for all classes, normalized by the average values achieved with the real dataset, CASIA-WebFace. VIGFace achieves superior scores in terms of class consistency, class separability, and intra-class diversity compared to other methods. SynFace exhibits the lowest separability due to its mix-up generation method. This fact indicates that SynFace can generate only a limited number of subjects as mentioned in the introduction. DigiFace achieves strong consistency, due to its 3D rendering methods, but its image style may differ significantly from real datasets, leading to lower accuracy in real-world applications. DCFace, the SOTA model that also utilizes a diffusion model, exhibits separability similar to that of VIGFace, but Fig. 5 illustrates that DCFace exhibits inferior uniformity in the same class. DCFace also demonstrates inadequate FIQA diversity, indicating limited variations in factors such as pose, lighting, and occlusion.

Originality from real human We also demonstrate that the generated identities represent non-existent humans by querying the most similar face in the CASIA-WebFace dataset. For comparison, we present the similarity values of the nearest negative class center in CASIA-WebFace. As shown in Fig. 6b, the top-1 similarity score for a real human is lower than the nearest negative class center similarity in CASIA-WebFace. This supports the claim that each synthesized image depicts a non-existent human face. In this paper, we avoid thresholding or selective sampling, which could harm fair comparisons with previous methods.

Method	Condition			Verification Benchmarks						IJB Benchmarks	
	Real Image	Synthetic Image		LFW	CFP-FP	CPLFW	AgeDB	CALFW	Avg.	IJB-B	IJB-C
		Real ID	Virtual ID								
CASIA-WebFace	✓			99.30	96.41	88.88	94.25	92.57	94.28	78.71	83.44
SynFace	✓		✓	99.32	96.19	88.62	93.35	92.55	94.01 (-0.27)	74.95 (-3.76)	80.36 (-3.08)
DigiFace	✓		✓	99.45	97.34	89.73	94.12	92.97	94.72 (+0.44)	78.47 (-0.24)	82.85 (-0.59)
DCFace	✓		✓	99.50	96.90	89.27	94.13	92.90	94.54 (+0.26)	78.34 (-0.37)	82.85 (-0.59)
iDiffFace	✓		✓	99.48	97.31	89.85	94.18	92.88	94.74 (+0.46)	77.42 (-1.29)	81.40 (-2.04)
GANDiffFace	✓		✓	99.50	96.99	89.32	93.48	92.70	94.40 (+0.12)	75.28 (-3.43)	79.55 (-3.89)
VIGFace(B)	✓		✓	99.52	97.73	89.97	95.00	93.12	95.07 (+0.79)	80.62 (+1.91)	85.59 (+2.15)
	✓	✓		99.35	97.20	89.37	93.68	92.98	94.52 (+0.24)	79.18 (+0.47)	84.02 (+0.58)
	✓	✓	✓	99.55	98.03	90.65	94.63	93.40	95.25 (+0.97)	80.81 (+2.10)	85.43 (+1.99)

Table 3. Augmented FR performance results for various condition of synthetic dataset. The accuracies (%) for LFW, CFP-FP, CPLFW, AgeDB-30, CALFW, and the average benchmark accuracies are reported. IJB is reported at TAR@FAR=1e-4. Red signifies enhanced outcomes compared to CASIA-WebFace, whereas Blue denotes a reduction in results.

4.3. Evaluation

VIGFace as Virtual Dataset We compare the performance of the FR model trained with generated facial images for virtual IDs using VIGFace with conventional methods: SynFace [38], DigiFace [2], DCFace [26], iDiff-Face [4], and GANDiffFace [33]. All datasets were obtained from the official GitHub repository released by the authors. For the experiment, we set the number of virtual IDs to 10K and 60K. To ensure a fair comparison, we established image counts of 0.5M and 1.2M, which represent the scale of the real CASIA-WebFace dataset and previous synthetic approaches, respectively. In Tab. 1, we present the 1:1 verification accuracy (%) on five benchmarks [20, 35, 41, 56, 57] and IJB [32, 53] datasets. From the table, it is evident that DCFace achieves a superior performance among conventional methods. However, VIGFace(B) outperforms the previous state-of-the-art method on every benchmark dataset. Notably, VIGFace(B) achieves equal or even better performance on CFP-FP and CPLFW compared to the model trained with the real dataset, CASIA-WebFace. This indicates that our method benefits from its pose-variable generation capabilities. As a result, when the FR model was trained using VIGFace, it achieves comparable performance to a model trained using a real dataset in terms of average accuracy. This suggests that our virtual dataset can serve as a full substitute for the CASIA-WebFace dataset in training the FR model, while avoiding privacy concerns.

To justify the effectiveness of the proposed VIGFace, we also assess its performance in diverse FR implementations. Tab. 2 compares DCFace, the previous state-of-the-art model, and VIGFace across various implementations. As shown in the table, VIGFace outperforms DCFace on most benchmarks, across different backbones (IR-SE50, IR-SE100) and methods (ArcFace [7], AdaFace [25]).

VIGFace as Data Augmentation To demonstrate the efficacy of VIGFace as an augmentation framework, we evaluate the accuracy of the FR model trained on both real and

synthetic images. Tab. 3 shows the performance change of the trained FR model utilizing various combinations of datasets. As depicted in the table, the FR model that is trained with a combination of real data and VIGFace exhibits enhanced performance on both verification and IJB benchmarks, compared to the model trained solely on real data. This is in contrast to more than one benchmark where the model exhibited a decline in performance when employing conventional synthetic datasets for augmentation. DigiFace [2] and iDiffFace [4] notably enhance FR results on verification benchmarks. However, DigiFace struggles to perform well on its own, devoid of real data, while iDiffFace significantly reduces IJB benchmark performance. This is due to their failure to precisely replicate the appearance of real-world facial images, making it impractical to present a privacy-free synthetic dataset. The results of our experiment indicate that the proposed method can accurately mirror the real facial data to blend and make synergy with them. In particular, augmented images of real IDs improve the results of the CFP-FP and CPLFW benchmarks. This observation suggests that the use of five-point facial landmarks in the conditioning method can create a variety of posed facial images, substantially improving the FR model’s ability to understand pose variations. Consequently, VIGFace not only effectively solves the privacy issue but can also be used with real data as part of the augmentation process. When trained with the VIGFace dataset, the FR backbone achieves better generalization and higher performance, in contrast to conventional methods, which are unable to achieve performance improvements.

Fig. 5 illustrates the results that synthesize variations of real and virtual IDs. Since the training process is significantly biased not just by a lack of subject but also by inner-class variance, increasing the variance within the class is crucial. The results demonstrate that the proposed approach can generate a variety of conditions for the existing real individuals without any help from external data. Since VIGFace can generate variance images of real individuals, we performed experiments on each type of augmentation, *i.e.*

synthetic images of real and virtual ID. In particular, we extend the long-tailed real-ID class, which contains fewer than 50 images, to 50 images. As can be seen in Tab. 3, the augmented dataset for real ID shows improved FR performance in most benchmarks. This fact indicates that our method can increase the intra-class diversity of the real dataset, a critical factor in achieving high FR performance. As a result, the FR model that utilizes the entire set of augmented data exhibits the best performance, benefiting from enhanced intra-class diversity and inter-class variance. Again, VIGFace proved its excellence in terms of not only the virtual dataset but also as a tool for augmentation methods.

5. Conclusions

This paper presents a simple yet effective method for creating a synthetic dataset that guarantees the unique virtual identities. Synthesized facial data can serve as a solution for various challenges faced by traditional real datasets, such as high expenses, inaccuracies and biases in labeling, and concerns regarding privacy. To this end, we propose the Virtual Identity Generation framework and demonstrate that it can generate not only realistic but also diverse facial images of virtual individuals, significantly narrowing the performance gap with FR models trained on real data. Furthermore, the model exhibits superior performance when trained on a combination of VIGFace and existing real data compared to models trained solely on real data. This confirms that our proposed method has potential as an effective augmentation technique. We will publicly distribute the virtual face dataset created by VIGFace and believe that these new virtual data will contribute to resolving the privacy issues inherent in face recognition training dataset.

References

- [1] Xiang An, Xuhan Zhu, Yuan Gao, Yang Xiao, Yongle Zhao, Ziyong Feng, Lan Wu, Bin Qin, Ming Zhang, Debing Zhang, et al. Partial fc: Training 10 million identities on a single machine. In *Proceedings of the IEEE/CVF International Conference on Computer Vision*, pages 1445–1449, 2021. 3
- [2] Gwangbin Bae, Martin de La Gorce, Tadas Baltrušaitis, Charlie Hewitt, Dong Chen, Julien Valentin, Roberto Cipolla, and Jingjing Shen. Digiface-1m: 1 million digital face images for face recognition. In *Proceedings of the IEEE/CVF Winter Conference on Applications of Computer Vision*, pages 3526–3535, 2023. 2, 3, 6, 8
- [3] Fadi Boutros, Naser Damer, Florian Kirchbuchner, and Arjan Kuijper. Elasticface: Elastic margin loss for deep face recognition. In *Proceedings of the IEEE/CVF conference on computer vision and pattern recognition*, pages 1578–1587, 2022. 3
- [4] Fadi Boutros, Jonas Henry Grebe, Arjan Kuijper, and Naser Damer. Idiff-face: Synthetic-based face recognition through fuzzy identity-conditioned diffusion model. In *Proceedings of the IEEE/CVF International Conference on Computer Vision*, pages 19650–19661, 2023. 2, 3, 6, 8
- [5] Ting Chen. On the importance of noise scheduling for diffusion models. *arXiv preprint arXiv:2301.10972*, 2023. 6
- [6] Hyunwoo Cho, Haesol Park, Ig-Jae Kim, and Junghyun Cho. Data augmentation of backscatter x-ray images for deep learning-based automatic cargo inspection. *Sensors*, 2021. 2
- [7] Jiankang Deng, Jia Guo, Niannan Xue, and Stefanos Zafeiriou. Arcface: Additive angular margin loss for deep face recognition. In *Proceedings of the IEEE/CVF conference on computer vision and pattern recognition*, pages 4690–4699, 2019. 1, 3, 4, 5, 7, 8
- [8] Jiankang Deng, Jia Guo, Yuxiang Zhou, Jinke Yu, Irene Kotsia, and Stefanos Zafeiriou. Retinaface: Single-stage dense face localisation in the wild. *arXiv preprint arXiv:1905.00641*, 2019. 5
- [9] Jiankang Deng, Jia Guo, Tongliang Liu, Mingming Gong, and Stefanos Zafeiriou. Sub-center arcface: Boosting face recognition by large-scale noisy web faces. In *Computer Vision—ECCV 2020: 16th European Conference, Glasgow, UK, August 23–28, 2020, Proceedings, Part XI 16*, pages 741–757. Springer, 2020. 1
- [10] Jiankang Deng, Jia Guo, Jing Yang, Alexandros Lattas, and Stefanos Zafeiriou. Variational prototype learning for deep face recognition. In *Proceedings of the IEEE/CVF Conference on Computer Vision and Pattern Recognition*, pages 11906–11915, 2021. 3
- [11] Yu Deng, Jialong Yang, Dong Chen, Fang Wen, and Xin Tong. Disentangled and controllable face image generation via 3d imitative-contrastive learning. In *Proceedings of the IEEE/CVF conference on computer vision and pattern recognition*, pages 5154–5163, 2020. 2, 3
- [12] Alexey Dosovitskiy, Lucas Beyer, Alexander Kolesnikov, Dirk Weissenborn, Xiaohua Zhai, Thomas Unterthiner, Mostafa Dehghani, Matthias Minderer, Georg Heigold, Sylvain Gelly, et al. An image is worth 16x16 words: Transformers for image recognition at scale. *arXiv preprint arXiv:2010.11929*, 2010. 3, 5
- [13] Yandong Guo, Lei Zhang, Yuxiao Hu, Xiaodong He, and Jianfeng Gao. Ms-celeb-1m: A dataset and benchmark for large-scale face recognition. In *Computer Vision—ECCV 2016: 14th European Conference, Amsterdam, The Netherlands, October 11–14, 2016, Proceedings, Part III 14*, pages 87–102. Springer, 2016. 1, 3
- [14] Kaiming He, Xiangyu Zhang, Shaoqing Ren, and Jian Sun. Delving deep into rectifiers: Surpassing human-level performance on imagenet classification. In *Proceedings of the IEEE international conference on computer vision*, pages 1026–1034, 2015. 1
- [15] Kaiming He, Xiangyu Zhang, Shaoqing Ren, and Jian Sun. Deep residual learning for image recognition. In *Proceedings of the IEEE conference on computer vision and pattern recognition*, pages 770–778, 2016. 1
- [16] Jonathan Ho and Tim Salimans. Classifier-free diffusion guidance. In *NeurIPS 2021 Workshop on Deep Generative Models and Downstream Applications*, 2021. 5, 6
- [17] Je Hyeong Hong, Hanjo Kim, Minsoo Kim, Gi Pyo Nam, Junghyun Cho, Hyeong-Seok Ko, and Ig-Jae Kim. A 3d

- model-based approach for fitting masks to faces in the wild. In *2021 IEEE International Conference on Image Processing (ICIP)*, 2021. 2
- [18] Jie Hu, Li Shen, and Gang Sun. Squeeze-and-excitation networks. In *Proceedings of the IEEE conference on computer vision and pattern recognition*, pages 7132–7141, 2018. 1
- [19] Gary Huang, Marwan Mattar, Honglak Lee, and Erik Learned-Miller. Learning to align from scratch. *Advances in neural information processing systems*, 25, 2012. 3, 5
- [20] Gary B Huang, Marwan Mattar, Tamara Berg, and Eric Learned-Miller. Labeled faces in the wild: A database for studying face recognition in unconstrained environments. In *Workshop on faces in 'Real-Life' Images: detection, alignment, and recognition*, 2008. 7, 8
- [21] Yuge Huang, Yuhan Wang, Ying Tai, Xiaoming Liu, Pengcheng Shen, Shaoxin Li, Jilin Li, and Feiyue Huang. Curricularface: adaptive curriculum learning loss for deep face recognition. In *proceedings of the IEEE/CVF conference on computer vision and pattern recognition*, pages 5901–5910, 2020. 3
- [22] Hochul Hwang, Cheongjae Jang, Geonwoo Park, Junghyun Cho, and Ig-Jae Kim. Eldersim: A synthetic data generation platform for human action recognition in eldercare applications. *IEEE Access*, 2023. 2
- [23] Sergey Ioffe and Christian Szegedy. Batch normalization: Accelerating deep network training by reducing internal covariate shift. In *International conference on machine learning*, pages 448–456. pmlr, 2015. 1
- [24] Ira Kemelmacher-Shlizerman, Steven M Seitz, Daniel Miller, and Evan Brossard. The megaface benchmark: 1 million faces for recognition at scale. In *Proceedings of the IEEE conference on computer vision and pattern recognition*, pages 4873–4882, 2016. 2
- [25] Minchul Kim, Anil K Jain, and Xiaoming Liu. Adaface: Quality adaptive margin for face recognition. In *Proceedings of the IEEE/CVF conference on computer vision and pattern recognition*, pages 18750–18759, 2022. 1, 3, 8
- [26] Minchul Kim, Feng Liu, Anil Jain, and Xiaoming Liu. De-face: Synthetic face generation with dual condition diffusion model. In *Proceedings of the IEEE/CVF Conference on Computer Vision and Pattern Recognition*, pages 12715–12725, 2023. 2, 3, 6, 8
- [27] D Kinga, Jimmy Ba Adam, et al. A method for stochastic optimization. In *International conference on learning representations (ICLR)*, page 6. San Diego, California., 2015. 6
- [28] Shanchuan Lin, Bingchen Liu, Jiashi Li, and Xiao Yang. Common diffusion noise schedules and sample steps are flawed. In *Proceedings of the IEEE/CVF winter conference on applications of computer vision*, pages 5404–5411, 2024. 5, 6
- [29] Weiyang Liu, Yandong Wen, Zhiding Yu, Ming Li, Bhiksha Raj, and Le Song. Sphreface: Deep hypersphere embedding for face recognition. In *Proceedings of the IEEE conference on computer vision and pattern recognition*, pages 212–220, 2017. 1, 3, 5
- [30] Yaojie Liu and Xiaoming Liu. Spoof trace disentanglement for generic face anti-spoofing. *IEEE Transactions on Pattern Analysis and Machine Intelligence*, 45(3):3813–3830, 2022. 3
- [31] Ilya Loshchilov and Frank Hutter. Decoupled weight decay regularization. *arXiv preprint arXiv:1711.05101*, 2017. 6
- [32] Brianna Maze, Jocelyn Adams, James A Duncan, Nathan Kalka, Tim Miller, Charles Otto, Anil K Jain, W Tyler Niggel, Janet Anderson, Jordan Cheney, et al. Iarpa janus benchmark-c: Face dataset and protocol. In *2018 international conference on biometrics (ICB)*, pages 158–165. IEEE, 2018. 8
- [33] Pietro Melzi, Christian Rathgeb, Ruben Tolosana, Ruben Vera-Rodriguez, Dominik Lawatsch, Florian Domin, and Maxim Schaubert. Gandifface: Controllable generation of synthetic datasets for face recognition with realistic variations. In *Proceedings of the IEEE/CVF International Conference on Computer Vision*, pages 3086–3095, 2023. 3, 6, 8, 2
- [34] Qiang Meng, Shichao Zhao, Zhida Huang, and Feng Zhou. Magface: A universal representation for face recognition and quality assessment. In *Proceedings of the IEEE/CVF conference on computer vision and pattern recognition*, pages 14225–14234, 2021. 3
- [35] Stylianos Moschoglou, Athanasios Papaioannou, Christos Sagonas, Jiankang Deng, Irene Kotsia, and Stefanos Zafeiriou. Agedb: the first manually collected, in-the-wild age database. In *proceedings of the IEEE conference on computer vision and pattern recognition workshops*, pages 51–59, 2017. 7, 8
- [36] Aaron Nech and Ira Kemelmacher-Shlizerman. Level playing field for million scale face recognition. In *Proceedings of the IEEE Conference on Computer Vision and Pattern Recognition*, pages 7044–7053, 2017. 2
- [37] William Peebles and Saining Xie. Scalable diffusion models with transformers. In *Proceedings of the IEEE/CVF International Conference on Computer Vision*, pages 4195–4205, 2023. 3, 5
- [38] Haibo Qiu, Baosheng Yu, Dihong Gong, Zhifeng Li, Wei Liu, and Dacheng Tao. Synface: Face recognition with synthetic data. In *Proceedings of the IEEE/CVF International Conference on Computer Vision*, pages 10880–10890, 2021. 2, 3, 6, 8
- [39] Swami Sankaranarayanan, Azadeh Alavi, Carlos D Castillo, and Rama Chellappa. Triplet probabilistic embedding for face verification and clustering. In *2016 IEEE 8th international conference on biometrics theory, applications and systems (BTAS)*, pages 1–8. IEEE, 2016. 1
- [40] Florian Schroff, Dmitry Kalenichenko, and James Philbin. Facenet: A unified embedding for face recognition and clustering. In *Proceedings of the IEEE conference on computer vision and pattern recognition*, pages 815–823, 2015. 1
- [41] Soumyadip Sengupta, Jun-Cheng Chen, Carlos Castillo, Vishal M Patel, Rama Chellappa, and David W Jacobs. Frontal to profile face verification in the wild. In *2016 IEEE winter conference on applications of computer vision (WACV)*, pages 1–9. IEEE, 2016. 7, 8
- [42] Karen Simonyan and Andrew Zisserman. Very deep convolutional networks for large-scale image recognition. *arXiv preprint arXiv:1409.1556*, 2014. 1

- [43] Jiaming Song, Chenlin Meng, and Stefano Ermon. Denoising diffusion implicit models. *arXiv preprint arXiv:2010.02502*, 2020. 6
- [44] Nitish Srivastava, Geoffrey Hinton, Alex Krizhevsky, Ilya Sutskever, and Ruslan Salakhutdinov. Dropout: a simple way to prevent neural networks from overfitting. *The journal of machine learning research*, 15(1):1929–1958, 2014. 1
- [45] Yiyou Sun, Yaojie Liu, Xiaoming Liu, Yixuan Li, and Wen-Sheng Chu. Rethinking domain generalization for face anti-spoofing: Separability and alignment. In *Proceedings of the IEEE/CVF Conference on Computer Vision and Pattern Recognition*, pages 24563–24574, 2023. 3
- [46] Philipp Terhörst, Jan Niklas Kolb, Naser Damer, Florian Kirchbuchner, and Arjan Kuijper. Ser-fiq: Unsupervised estimation of face image quality based on stochastic embedding robustness. In *CVPR*, page 2, 2020. 7
- [47] Jonathan Tremblay, Aayush Prakash, David Acuna, Mark Brophy, Varun Jampani, Cem Anil, Thang To, Eric Cameracci, Shaad Boochoon, and Stan Birchfield. Training deep networks with synthetic data: Bridging the reality gap by domain randomization. In *Proceedings of the IEEE conference on computer vision and pattern recognition workshops*, pages 969–977, 2018. 2
- [48] Boris van Breugel, Trent Kyono, Jeroen Berrevoets, and Mihaela van der Schaar. Decaf: Generating fair synthetic data using causally-aware generative networks. *Advances in Neural Information Processing Systems*, 34:22221–22233, 2021. 2
- [49] Laurens Van der Maaten and Geoffrey Hinton. Visualizing data using t-sne. *Journal of machine learning research*, 9(11), 2008. 2
- [50] Richard Van Noorden. The ethical questions that haunt facial-recognition research. *Nature*, 587(7834):354–359, 2020. 2
- [51] Hao Wang, Yitong Wang, Zheng Zhou, Xing Ji, Dihong Gong, Jingchao Zhou, Zhifeng Li, and Wei Liu. Cosface: Large margin cosine loss for deep face recognition. In *Proceedings of the IEEE conference on computer vision and pattern recognition*, pages 5265–5274, 2018. 3
- [52] Yandong Wen, Kaipeng Zhang, Zhifeng Li, and Yu Qiao. A discriminative feature learning approach for deep face recognition. In *Computer Vision—ECCV 2016: 14th European Conference, Amsterdam, The Netherlands, October 11–14, 2016, Proceedings, Part VII 14*, pages 499–515. Springer, 2016. 1
- [53] Cameron Whitelam, Emma Taborsky, Austin Blanton, Brianna Maze, Jocelyn Adams, Tim Miller, Nathan Kalka, Anil K Jain, James A Duncan, Kristen Allen, et al. Iarpa janus benchmark-b face dataset. In *proceedings of the IEEE conference on computer vision and pattern recognition workshops*, pages 90–98, 2017. 8
- [54] Dong Yi, Zhen Lei, Shengcai Liao, and Stan Z Li. Learning face representation from scratch. *arXiv preprint arXiv:1411.7923*, 2014. 1
- [55] Kaipeng Zhang, Zhanpeng Zhang, Zhifeng Li, and Yu Qiao. Joint face detection and alignment using multitask cascaded convolutional networks. *IEEE signal processing letters*, 23(10):1499–1503, 2016. 5
- [56] Tianyue Zheng and Weihong Deng. Cross-pose lfw: A database for studying cross-pose face recognition in unconstrained environments. *Beijing University of Posts and Telecommunications, Tech. Rep.*, 5(7), 2018. 7, 8
- [57] Tianyue Zheng, Weihong Deng, and Jiani Hu. Cross-age lfw: A database for studying cross-age face recognition in unconstrained environments. *arXiv preprint arXiv:1708.08197*, 2017. 7, 8
- [58] Zheng Zhu, Guan Huang, Jiankang Deng, Yun Ye, Junjie Huang, Xinze Chen, Jiagang Zhu, Tian Yang, Jiwen Lu, Da-long Du, et al. Webface260m: A benchmark unveiling the power of million-scale deep face recognition. In *Proceedings of the IEEE/CVF Conference on Computer Vision and Pattern Recognition*, pages 10492–10502, 2021. 1, 3

VIGFace: Virtual Identity Generation for Privacy-Free Face Recognition

Supplementary Material

Training Dataset	# of Images		Verification Benchmarks						IJB Benchmarks	
	classes	variations	LFW	CFP-FP	CPLFW	AgeDB	CALFW	Avg.	IJB-B	IJB-C
CASIA-Webface (Real)	≈ 10.5K	× 47	99.30	96.41	88.88	94.25	92.57	94.28	78.71	83.44
VIGFace (S)	10K	× 50	98.60	94.74	85.47	88.60	88.52	91.19	62.22	69.27
VIGFace (B)	60K	× 20	99.10	96.47	88.82	92.32	92.15	93.77	72.68	78.85
		× 50	99.25	96.99	89.25	93.23	92.25	94.19	75.00	80.90
VIGFace (L)	120K	× 20	99.15	96.54	89.62	92.75	92.25	94.06	75.11	80.65
		× 50	99.20	96.70	89.93	92.43	92.18	94.09	75.17	80.84

Table 4. Performance results of the FR model trained with differing sizes of virtual IDs and variations.

A. Impact of the quantity of classes and images

In this section, we generate VIGFace to have a different number of subjects and its variations, to investigate the effect of intra-class and inter-class diversity. As shown in Tab. 4, generally, increasing the number of virtual subjects and images leads to better FR performance. Our method, with 60K subjects and 50 variations, achieved an average score of 94.19 on five benchmarks, with only a 0.09 gap compared to the model trained on a real dataset, without any additional training data. This model also achieved remarkably high performance on IJB-B and IJB-C, with only 3.71 and 2.54 gaps, respectively, compared to the FR backbone trained on a real dataset. However, we observed that generating more than 60K subjects does not achieve remarkable performance gains, indicating saturation.

B. Stage 1 : FR model performance employing virtual prototypes

We evaluate the performance of the trained backbone achieved at the end of stage 1. Given that our approaches employ virtual prototypes, it is essential to guarantee that the virtual prototype does not affect the FR backbone training. As can be seen in Tab. 5, our approach maintains the benchmark face recognition performance with negligible changes.

Training Dataset	Real Prototype	Virtual Prototype	Average Accuracy	IJB-B	IJB-C
CASIA-Webface	10.5K	-	94.28	78.71	83.44
		60K	94.30	79.07	83.46

Table 5. Benchmark results of the stage 1: FR model which employs different number of virtual prototypes.

C. Specific benchmark comparison with the conventional SOTA method

Tab. 6 shows the specific five popular FR verification benchmark performance compared to the conventional state-of-the-art model, DCFace. As can be seen in the table, VIGFace(B) achieves significantly better performance on CFP-FP and CPLFW compared to the model trained with the DCFace. This indicates that the use of our synthetic dataset provides substantial advantages in handling pose variation capabilities. Additionally, our method achieved better performance compared to DCFace on the AgeDB and CALFW benchmarks, demonstrating that it is also effective in generating virtual identities with various age variations. As a result, VIGFace showcases its effectiveness by achieving superior performance compared to the previous SOTA method across all benchmarks.

D. Augmentation performance with large-scale VIGFace (L)

We evaluate the FR model trained on real and synthetic images of VIGFace (L). As shown in Tab. 7, the FR model that utilizes the entire set of augmented data from the large-scale VIGFace (L) exhibits the superior performance. Specifically, the model trained with dataset that is augmented by VIGFace (L) is improved 1.67 on average of five benchmarks and also achieves a performance improvement remarkably 6.46, 5.65 on IJB-B and IJB-C, respectively. This implies that face recognition models may gain advantages from the massive intra-class diversity and inter-class variance of large-scale VIGFace (L).

E. Example samples from failure case

In this section, we compare the failure case in terms of three important properties of datasets, which are consistency, sep-

Condition				Verification Benchmarks					
Dataset	# of Images	Backbone	Method	LFW	CFP-FP	CPLFW	AgeDB	CALFW	Avg.
DCFace	1.2M	R50	ArcFace	98.42	86.37	82.13	90.25	90.88	89.61
		R50	AdaFace	98.85	87.83	83.50	91.53	91.80	90.70
		R100	ArcFace	98.27	87.16	82.37	90.43	91.12	89.87
		R100	AdaFace	98.97	88.63	83.67	91.63	91.93	90.97
VIGFace(B)	1.2M	R50	ArcFace	99.15	96.66	88.88	92.73	92.22	93.93
		R50	AdaFace	99.20	96.64	89.53	92.87	92.48	94.14
		R100	ArcFace	99.33	97.06	89.55	93.13	92.67	94.35
		R100	AdaFace	99.22	97.06	90.27	93.75	92.48	94.56

Table 6. Specific five popular FR verification benchmark performance. We compare VIGFace(B) results with conventional state-of-the-arts model, DCFace.

Condition				Verification Benchmarks						IJB Benchmarks	
Method	Real Image	Synthetic Image		LFW	CFP-FP	CPLFW	AgeDB	CALFW	Avg.	IJB-B	IJB-C
		Real ID	Virtual ID								
CASIA-WebFace	✓			99.30	96.41	88.88	94.25	92.57	94.28	78.71	83.44
VIGFace(B)	✓		✓	99.52	97.73	89.97	95.00	93.12	95.07 (+0.79)	80.62 (+1.91)	85.59 (+2.15)
	✓	✓		99.35	97.20	89.37	93.68	92.98	94.52 (+0.24)	79.18 (+0.47)	84.02 (+0.58)
	✓	✓	✓	99.55	98.03	90.65	94.63	93.40	95.25 (+0.97)	80.81 (+2.10)	85.43 (+1.99)
VIGFace(L)	✓	✓	✓	99.65	98.31	92.22	95.42	94.15	95.95 (+1.67)	85.17 (+6.46)	89.09 (+5.65)

Table 7. Augmented FR performance results for various condition of synthetic dataset. Average accuracy(%) of LFW, CFP-FP, CPLFW, AgeDB-30 and CALFW benchmarks is reported. IJB is reported on TAR@FAR=1e-4. Red indicates the improved performance gap compared to the performance of the model that was trained only on the real data set.

arability, and diversity. We sample images from the lowest 5% subjects of each property to illustrate the effectiveness of VIGFace in the failure case.

E.1. Subjects exhibit the lowest consistency

Fig. 7 shows the failure case images generated by conventional methods [2, 4, 26, 33, 38] and our methods. We report virtual subjects that exhibit the lowest 5% class consistency in each dataset. In other words, the depicted subjects have a propensity for label-flip bias. As illustrated in the figure, VIGFace demonstrates outstanding consistency while maintaining high diversity in image conditions. This suggests a minimal risk of label-flip bias and supports effective FR training. DigiFace also maintains high consistency, as it is based on 3D modeling. However, since the appearance of the DigiFace dataset does not align with real face images, the performance of an FR backbone trained on DigiFace is considerably subpar for real-world use cases.

E.2. Subjects exhibit the lowest separability

Fig. 8 shows the failure case images generated by conventional [2, 4, 26, 33, 38] and our methods. We report virtual subjects among those exhibiting the highest 5% cosine similarity. Generating overly similar or identical objects can result in label-noised data and negatively impact FR training. As shown in the figure, conventional methods often generate output that resembles the same object. This indicates

a lack of the ability to generate entirely novel individuals. For example, SynFace samples exhibit high similarities between objects because they utilize a mix-up to generate face images. As GANDiffFace depends on StyleGAN for creating virtual identities, it demonstrates limited capability in producing new subjects.

E.3. Subjects exhibit the lowest diversity

Fig. 9 shows the failure case images generated by conventional [2, 4, 26, 33, 38] and our methods. We report virtual subjects among those who exhibit the lowest 5% intra-class diversity in each dataset. Note that intra-class diversity does not pertain to changes in identity but relates to challenges such as variations in pose, lighting conditions, occlusion, and resolution. Since calculating diversity uses FIQA methods that measure how challenging the generated face images are for recognition, the diversity score may differ slightly from human perception. Still, we found that most of the generated subjects with low diversity contain only high-quality front-facing faces, which are easily recognizable in face recognition. However, even low-diversity subjects generated with VIGFace have high-quality images while maintaining diverse variations, such as pose or lighting. This is because VIGFace utilizes a diffusion model incorporating with landmark guidance, and each subject can have high-pose variations.



Figure 7. Low consistency subjects generated with various methods. Each row presents samples from the same ID that exhibits the lowest 5% consistency. The class consistency of each ID is indicated in the bottom-right corner.



Figure 8. Low separability subjects generated with various methods. Each row presents samples from the top 5% most similar subject pairs, with the cosine similarity between the two subjects indicated.

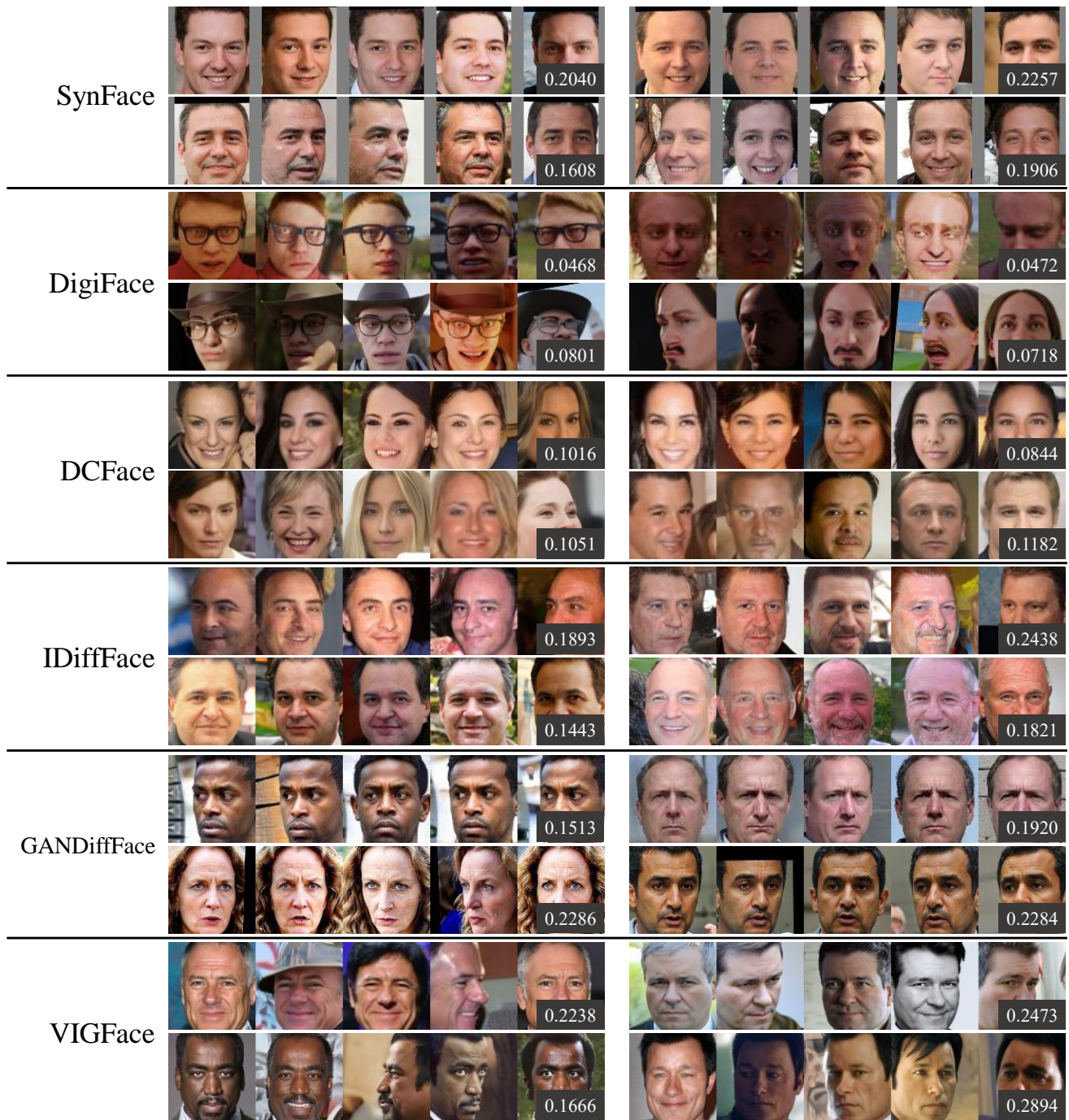


Figure 9. Low diversity subjects generated with various methods. Each row presents samples from the same ID that exhibits the lowest 5% diversity. The class diversity of each ID is indicated in the bottom-right corner.